Proceedings of the 7th International Conference on Asian and Pacific Coasts (APAC 2013) Bali, Indonesia, September 24-26, 2013

PREDICTION OF TOPOGRAPHIC CHANGES OF A CIRCULAR SANDY ISLAND USING BG MODEL

S. Miyahara [1], T. Uda [2] and M. Serizawa [1]

ABSTRACT: The BG model (a three-dimensional model for predicting beach changes based on Bagnold's concept) was applied to predict the three-dimensional topographic changes of a sandy island due to waves, which were observed in a movable-bed experiment by Uda and Yamamoto (1991). Taketomi Island in the Sea of Okhotsk was formed as an island composed of sand by a volcanic eruption, then the island was markedly deformed by wave action, resulting in the formation of a double tombolo behind the island (Zenkovich, 1967). The BG model was also applied to predict these topographic changes of the island. The predicted and measured topographic changes in the two examples were in good agreement.

Keywords: Circular island, beach changes, BG model, volcanic island, double tombolo

INTRODUCTION

An island composed of ash and pumice produced by volcanic eruptions may be rapidly deformed under wave action after its formation. Considering the shape of such an island to be a circle, when waves are incident to the island, sand is transported from the exposed side of the island toward the lee side. In this case, the angle between the normal to the shoreline and the wave incidence will inevitably exceed 45° at a point along the circular shoreline because the direction normal to the shoreline differs by 180° between the side exposed to waves and the lee of the island. Thus, shoreline instability (Ashton et al., 2001) will occur in the calculation of beach changes using the ordinary longshore sand transport formula, making it difficult to obtain a stable solution.

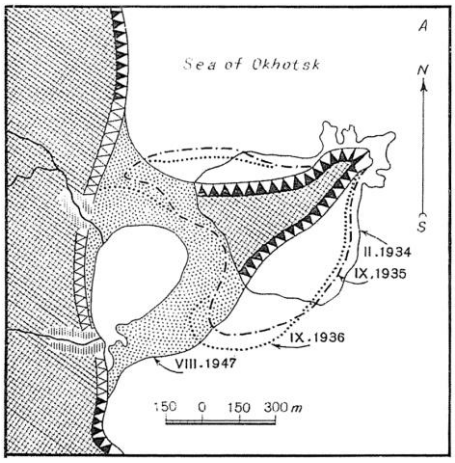

Fig. 1 Deformation of a volcanic island, Taketomi Island, formed 600 m offshore of Alaid Island in Okhotsk Sea (Zenkovich, 1967)

We have already proposed the BG model (a predictive model for the three-dimensional (3-D) beach changes based on Bagnold's concept), and its applicability for predicting various types of beach changes has been confirmed (Serizawa and Uda, 2011). In this study, we apply our model to predict the beach changes of an island composed of sand under wave action. First, the model was validated using the experimentally observed changes of a sandy island reported by Uda and Yamamoto (1991). Then, topographic changes of an island recently formed by volcanic eruptions in the Okhotsk Sea and the formation of a double tombolo around the island were predicted using this model.

DEFORMATION OF CIRCULAR ISLAND COMPOSED OF UNCONSOLIDATED MATERIALS

Figure 1 shows the erosion of an island recently formed by volcanic eruptions in the Okhotsk Sea and the formation of a double tombolo in the lee of the island (Zenkovich, 1967). In 1933, a volcanic island, Taketomi Island, was formed 600 m offshore of Alaid Island in the Okhotsk Sea. Because this island was composed of unconsolidated materials such as ash and pumice, it was rapidly eroded after formation, and a couple of sand bars started to extend behind the island. These sand bars extended toward Alaid Island until 1936 with a velocity of 300 m/yr in the sea with 25 m depth, and approached very close to the island. Then, the two sand bars connected the two islands from 1936 to 1947, leaving a lagoon between them.

[1] Coastal Engineering Laboratory Co., Ltd., 1-22-301 Wakaba, Shinjuku, Tokyo 160-001, JAPAN
[2] Public Works Research Center, 1-6-4 Taito, Taito, Tokyo 110-0016, JAPAN

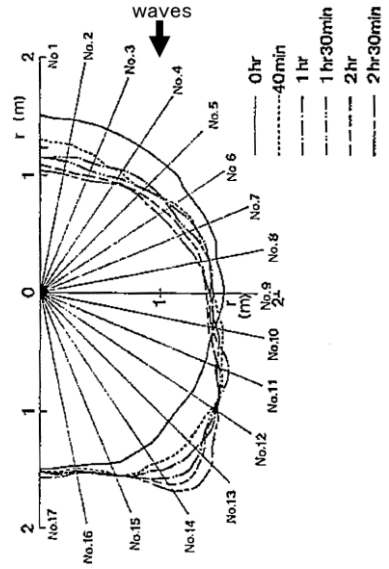

Fig. 2 Shoreline changes of a semicircular island composed of sand

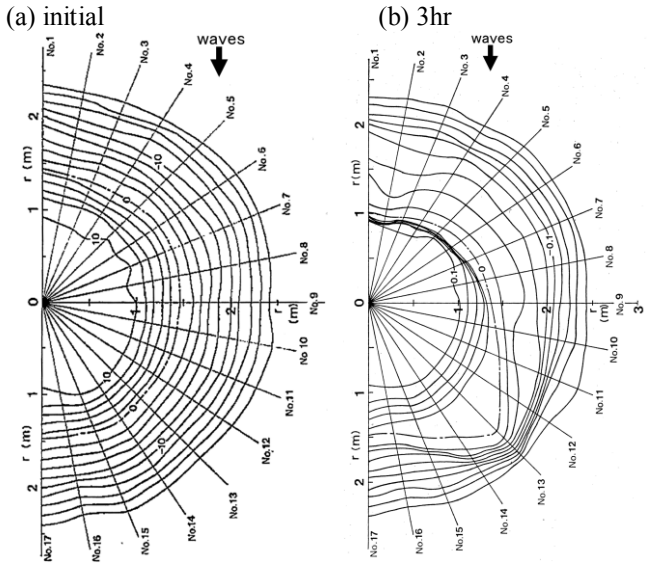

Fig. 3 Initial bathymetry with semicircular contours and resulting bathymetry after 3 hr wave generation

EXPERIMENT OF DEFORMATION OF SANDY ISLAND

Uda and Yamamoto (1991) investigated the beach changes around a circular island composed of sand by performing a movable-bed experiment. We used their results as the data set for validating the applicability of the BG model. The model circular island in their experiment was produced using fine sand of median diameter 0.28 mm. The initial beach slope was set to 1/5 and the initial shoreline was given by a semicircle with a radius of 1.5 m, taking the symmetry of the island into account. The island initially consisted of a semicircular plane with 10 cm height above mean sea level, and the water depth surrounding the island was 20 cm. Incident waves with a height of 3 cm and a wave period of 0.8 s were generated, and beach changes were measured along 16 transects arranged in radial directions around the semicircular island.

Figure 2 shows the shoreline changes in the first 3 hr. The shoreline retreated upcoast of transect No. 10, whereas it advanced downcoast of transect No. 10. The velocity of shoreline recession in the erosion zone was large in the earlier stages and the rate of the shoreline change decreased over time. In the area downcoast of transect No. 10, the shoreline protruded furthest between transect Nos. 13 and 14, and a cuspate foreland gradually developed with increasing curvature of the shoreline. As a result of the deformation, the symmetrical shoreline became asymmetric.

Figures 3(a) and 3(b) show the initial bathymetry with semicircular contours and the resulting bathymetry after 3 hr wave generation, respectively. Comparing both figures, it is clear that erosion occurred between transect Nos. 1 and 10, whereas sand was deposited between transect Nos. 10 and 16. In the erosion zone, the interval of the contours between the shoreline and the depth of closure of approximately 8 cm depth increased, resulting in the formation of a gently sloping offshore seabed. In contrast, a scrap was formed on the land and the interval between contours markedly decreased. In the accretion zone, beach changes occurred at depths greater than those in the erosion zone because of sand falling into the offshore zone, and the beach slope at the tip of the cuspate foreland became as steep as 1/1.5, which is the slope corresponding to the angle of repose, whereas a wide flat foreshore was formed on the land owing to the successive deposition of sand.

PREDICTIVE MODEL

In this study we used the BG model proposed by Serizawa and Uda (2011), which includes the Ozasa and Brampton (1980) term to evaluate the additional longshore sand transport induced by the longshore gradient of the breaker height. The fundamental equations are

$$\vec{q}=C_0\frac{P}{\tan\beta_c}\left\{\begin{array}{l}K_n\left(\tan\beta_c\vec{e_w}-|\cos\alpha|\,\overrightarrow{\nabla Z}\right)\\+\left\{(K_s-K_n)\sin\alpha-\dfrac{K_2}{\tan\beta}\dfrac{\partial H}{\partial s}\right\}\tan\beta\vec{e_s}\end{array}\right\} \quad (-h_c\le Z\le h_R) \tag{1}$$

$$P=\rho u_m^3 \tag{2}$$

$$u_m=\frac{H}{2}\sqrt{\frac{g}{h}} \tag{3}$$

Here, $\vec{q}=(q_x,q_y)$ is the net sand transport flux, Z (x, y, t)

is the elevation, n and s are the local coordinates taken along the directions normal (shoreward) and parallel to the contour lines, $\overrightarrow{\nabla Z}=(\partial Z/\partial x, \partial Z/\partial y)$ is the slope vector, $\vec{e}_w$ is the unit vector in the wave direction, $\vec{e}_s$ is the unit vector parallel to the contour lines, α is the angle between the wave direction and the direction normal to the contour lines, $\tan\beta=|\overrightarrow{\nabla Z}|$ is the seabed slope, $\tan\beta_c$ is the equilibrium slope, $\tan\beta \vec{e}_s=(-\partial Z/\partial y, \partial Z/\partial x)$, K_s and K_n are the coefficients of longshore sand transport and cross-shore sand transport, K_2 is the coefficient of the term given by Ozasa and Brampton (1980), $\partial H/\partial s=\vec{e}_s\cdot\overrightarrow{\nabla H}$ is the longshore gradient of the wave height H measured parallel to the contour lines, and $\tan\beta$ is the characteristic slope of the breaker zone, respectively. In addition, C_0 is the coefficient transforming an expression in terms of the immersed weight into a volumetric expression ($C_0=1/\{(\rho_s-\rho)g(1-p)\}$, where ρ is the density of seawater, ρ_s is the specific gravity of sand particles, p is the porosity of sand, and g is acceleration due to gravity), u_m is the seabed velocity due to the orbital motion of waves given by Eq. (3), h_c is the depth of closure, and h_R is the berm height.

The wave field was calculated using the energy balance equation given by Mase (2001) with the energy dissipation term due to wave breaking (Dally et al., 1984). Because repeated feedback calculations are necessary in response to the topographic changes in this calculation, the energy balance equation was used to reduce the calculation load, and the regular wave conditions in the experiment were replaced by the irregular wave conditions. In the calculation of the wave field on land, the imaginary depth h' (given by Eq. (4)) between the minimum depth h_0 and the berm height h_R was considered similarly to in the ordinary model for predicting 3-D beach changes.

$$h'=\left(\frac{h_R-Z}{h_R+h_0}\right)^{\mathrm{r}} h_0 \quad (\mathrm{r}=1) \quad (-h_0\le Z\le h_R) \tag{4}$$

The wave energy was set to 0 in the area with the elevation higher than the berm height. The calculation of the wave field was carried out every 10 steps of the calculation of the topographic changes. Wave incidence from the direction normal to the island was assumed in the same manner as in the experiment. The depth of closure h_c was assumed to be $2.5H$, where H is the wave height at a local point. The space scale in the calculation was set to 100 times that in the experiment, and then the calculation results were reduced by a scale of 1/100. The berm height was set to 2 m, and the equilibrium slope and the slope corresponding to the angle of repose were 1/5 and 1/2, respectively. The calculation domain was divided by a mesh of 20 m intervals in the longshore and cross-shore directions, and the calculation was carried out for 1000 hrs (5×10^5 steps) with a time interval of $\Delta t = 2\times10^{-3}$ hr. Table 1 shows the calculation conditions. In the case of the deformation of Taketomi Island, a circular island was assumed and the incident wave height H_i = 3 m and wave period T = 8 s were assumed, with the wave incidence from the direction normal to the average coastline.

Table 1 Calculation conditions.

Wave conditions	Incident waves: H_I = 3 m (0.3 cm), T = 8 s (0.8 s), wave direction θ_I = 0°relative to normal to initial shoreline
Berm height	h_R = 2 m (2 cm)
Depth of closure	$h_c = 2.5H$ (H: wave height)
Equilibrium slope	$\tan\beta_c$ = 1/5
Angle of repose slope	$\tan\beta_g$ = 1/2
Coefficients of sand transport	Coefficient of longshore sand transport K_s = 0.040 Coefficient of Ozasa and Brampton (1980) term $K_2 = 1.62K_s$ Coefficient of cross-shore sand transport $K_n = 0.1K_s$
Mesh size	$\Delta x = \Delta y$ = 20 m
Time interval	Δt = 0.002 h (0.0002h)
Duration of calculation	1000 hrs (5×10^5 steps)
Boundary conditions	Shoreward and landward ends: q_x = 0, right and left boundaries: q_y = 0
Calculation of wave field	Energy balance equation (Mase, 2001) ·Term of wave dissipation due to wave breaking: Dally et al. (1984) model ·Wave spectrum of incident waves: directional wave spectrum density obtained by Goda (1985) ·Total number of frequency components N_F = 1 and number of directional subdivisions N_θ = 8 ·Directional spreading parameter S_{max} = 75 ·Coefficients of wave breaking K = 0.17 and Γ = 0.3 ·Imaginary depth between minimum depth h_0 and berm height h_R : h_0 = 1 m (1 cm) ·Wave energy = 0 where $Z \ge h_R$ ·Lower limit of h in terms of wave decay due to breaking Φ: 1 m (1 cm)
Remarks	Numbers in parentheses show experimental values. Space and time scales in the calculation are 100- and 10-fold those in the experiment, respectively.

APPLICATION TO RESULTS OF MOVABLE-BED EXPERIMENT

Given a circular island, as shown in Fig. 4(a), as the initial condition similarly in the experiment, the topographic changes were predicted for the case of waves with a height of 3 cm and a period of 0.8 s

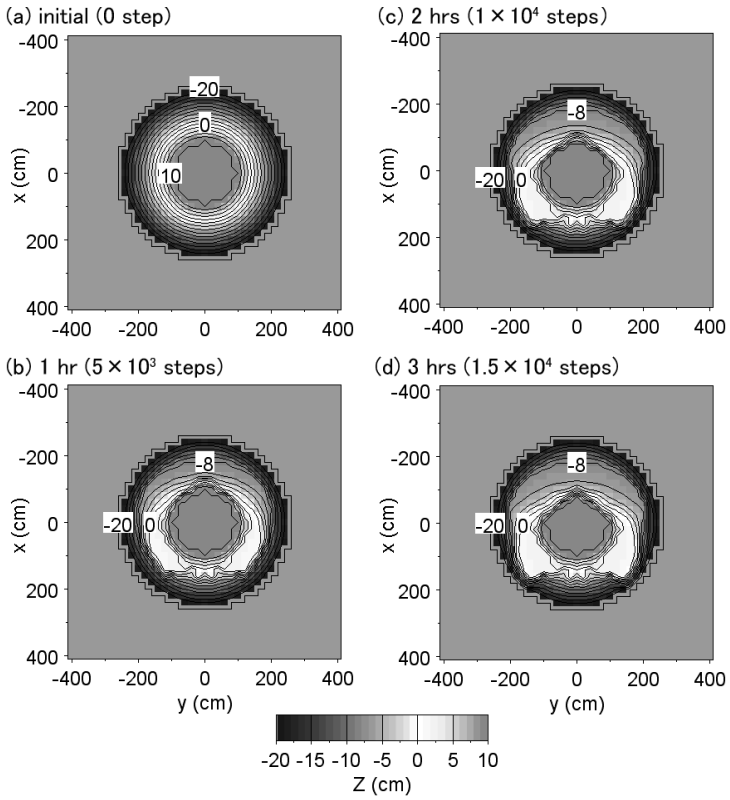

Fig. 4 Prediction of deformation of circular island based on results by movable-bed experiment

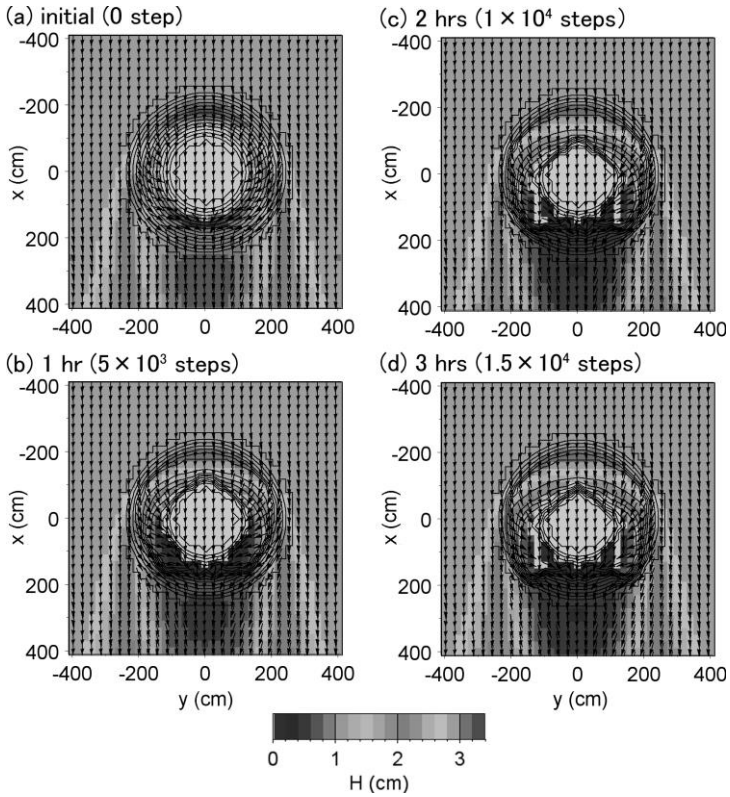

Fig. 5 Changes in wave field with time

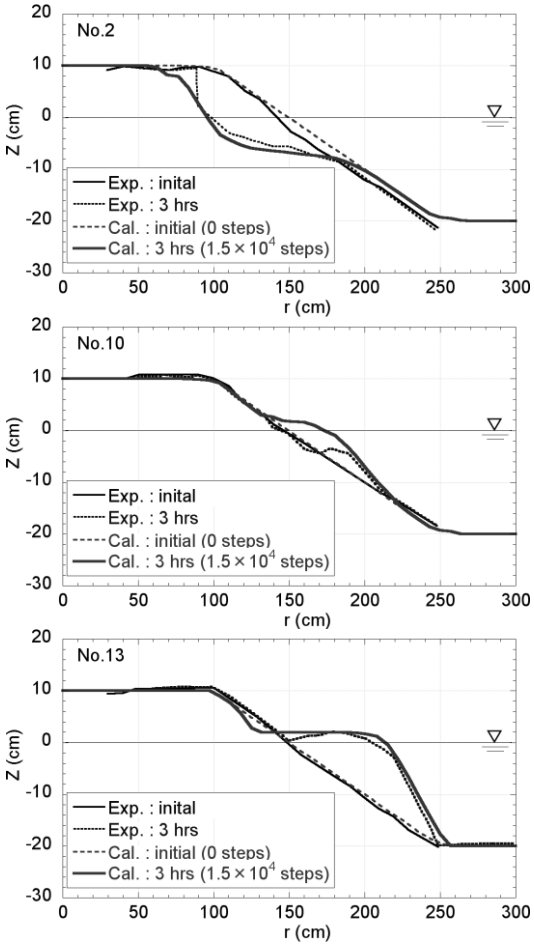

Fig. 6 Predicted and measured changes in longitudinal profiles.

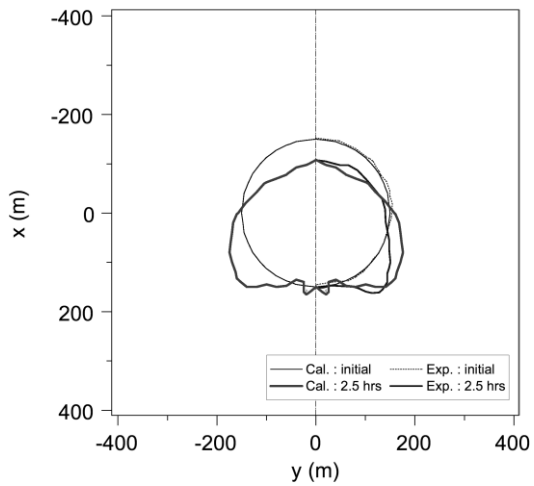

Fig. 7 Measured and predicted shorelines after 2.5 hrs.

incident from the *x*-direction. Under these wave conditions, longshore sand transport from the exposed side of the island to its lee was generated, resulting in erosion on the exposed side of the island. Sand supplied from the erosion zone was transported to the lee of the island, resulting in sand deposition. After 1 hr, a large

amount of sand had been deposited in the zone ranging between (= 117° and 138° with respect to the *x*-axis and cuspate forelands had formed, as shown in Fig. 4(b). Note that a flat plane foreshore with an extremely steep foreshore slope of 1/2 was formed by the successive deposition of sand due to the falling of sand in the deeper zone while maintaining the angle of repose of the sand.

After 2 hrs, the beach on the exposed side of the island had severely eroded, so that the shorelines intersected each other with an apex angle of 114°, whereas the sand deposition zone extended upcoast with the further protrusion and increase in the area of the cuspate forelands (Fig. 4(c)). After 3 hrs, the shoreline with an apex on the side exposed to waves had started to retreat and a couple of cuspate forelands had developed in the lee of the island because of the successive deposition of sand transported from the side exposed to waves (Fig. 4(d)). In contrast, a wave-cut terrace had formed in the offshore zone by erosion on the exposed side of the island because sand was transported away by longshore sand transport. Figure 4(d) corresponds to the experimental results shown in Fig. 3, which are in good agreement.

The wave field markedly changed with the changes in topography. Figure 5 shows the distribution of the wave height and wave direction under the initial conditions and after 1, 2 and 3 hrs. In the lee of the island, waves are obliquely incident to the shoreline, causing longshore sand transport from the exposed side to the lee of the island. Also a wave-shelter zone was formed in the lee of the island and the wave height decreased over time with the formation of the cuspate forelands in the lee of the island.

Figure 6 shows the measured and predicted changes in the cross-shore profiles in the erosion and accretion zones after 3 hrs. In the erosion zone, a gentle slope was formed offshore of the shoreline, whereas the land was cut by a steep slope to form a scarp. In the accretion zone, the shoreline markedly advanced forming a flat foreshore, and a steep slope with a slope of 1/2 was formed by sand falling sand into the deeper zone. These results were accurately predicted by the model. Along transect No. 10, located at the boundary between the erosion and accretion zones, a subsurface sand bar was formed in the experiment, whereas the emergence of a sand bar occurred in the calculation because a large amount of sand was deposited there, suggesting that the predicted volume of sand was slightly overestimated.

Figure 7 shows the predicted shoreline configuration after 2.5 hrs based on the experimental results shown in Fig. 2. The formation of cuspate forelands behind the island was predicted well, although the cuspate forelands extended further upcoast than in the experiment. Although there is some difference between the measured and predicted bathymetries, it was possible to quantitatively predict the topographic changes of a circular island.

SIMULATION OF DEFORMATION OF TAKETOMI ISLAND

The BG model was used to predict the deformation of Taketomi Island, the volcanic island investigated by Zenkovich (1967). Because the bathymetry around this island is unknown, direct application of the model to this island is not possible. Therefore, it was applied to the deformation of a circular island given the same boundary conditions as those of Taketomi Island. The coast of the main island on the opposite shore of Taketomi Island consists of cliffs with no sandy beach, as shown in Fig. 1, and therefore, a vertical wall was used to model the sea cliffs, as shown in Fig. 8(a), assuming zero sand transport across the wall and no reflection from the wall.

The results of the calculation are shown in Figs. 8(b) - 8(f). The pair of sand bars behind the island continued to develop in the direction of wave propagation, and the tip of the sand bars reached the sea cliff behind the island after 150 hrs, leaving a lagoon between them. After 250 hrs, because sand transport in the *x*-direction was blocked at the tip of the elongated sand bars, sand started to be transported along the wall. After 500 hrs, the width of the sand bars connecting the land increased. After 1000 hrs, the shape of the sand deposition zone resembled a bell. Once the sand bars reached the land, the topographic changes inside the lagoon ceased because of the lack of wave action, and the bathymetry immediately after its formation was maintained. On the other hand, most of the sandy island was eroded while forming a gently sloping seabed.

The changes in the longitudinal profiles across transect y = 0 m, dividing the island in two, and along transect x = 250 m, where the island is connected to the land, are shown in Fig. 9. The foreshore and shoreline retreated over time according to the longitudinal profile across transect y = 0 m, and a gentle slope of 1/40 was formed in the offshore zone. The water depth above the gentle seabed slope formed by erosion decreases landward, causing wave decay toward the shore, and resulting in a decrease in the depth of closure h_c. This explains why the gentle seabed slope was formed. Along transect x = 250 m, sand bars emerged owing to sand deposition over the flat seabed with a uniform depth of 5 m. Although quantitative simulation of the deformation of Taketomi Island is impossible because of lack of information of the bathymetry and wave conditions, the extension of sand bars from Taketomi Island to Alaid

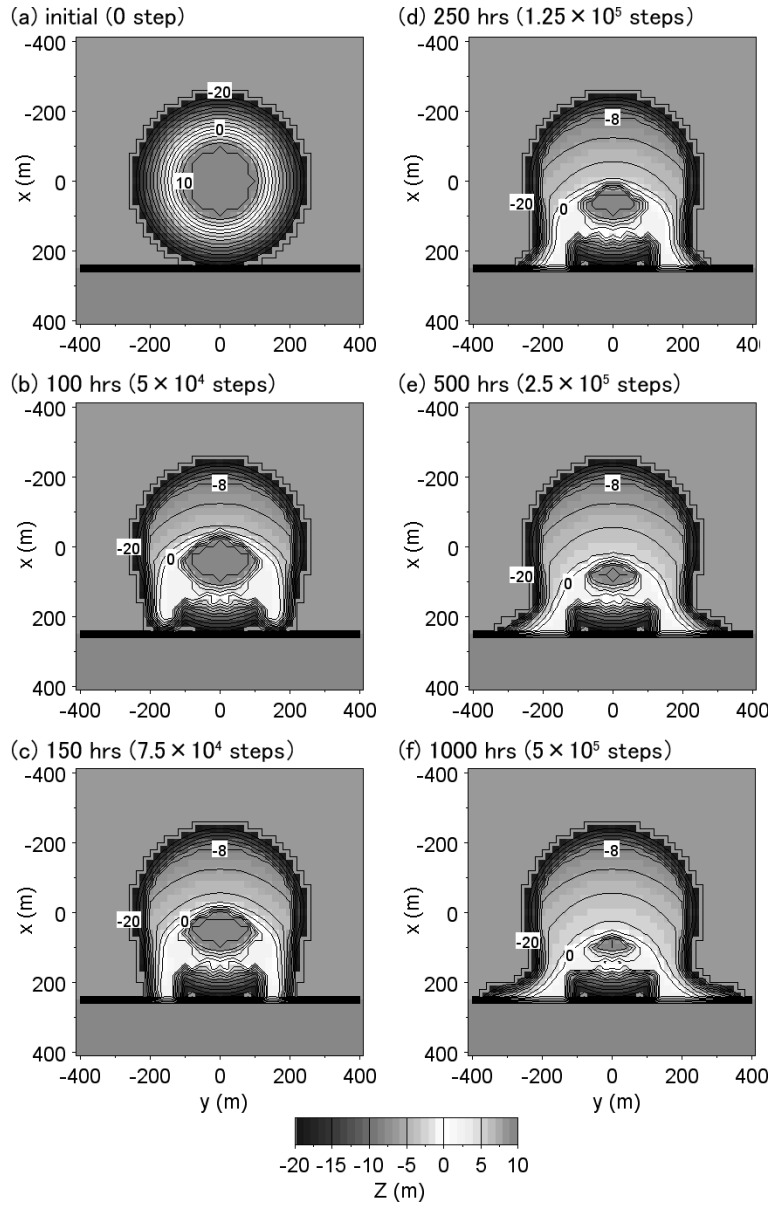

Fig. 8 Deformation of an island used to model Taketomi Island

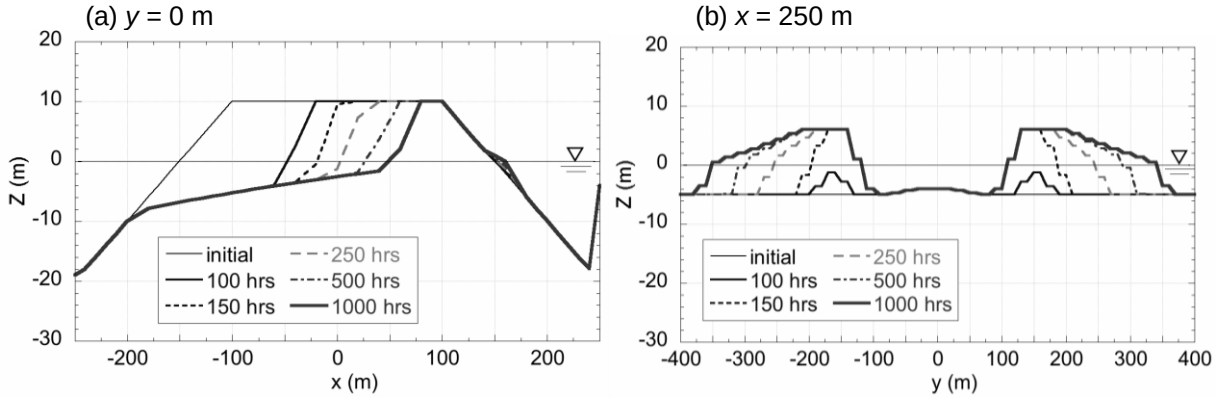

Fig. 9 Topographic changes along transects y = 0 m and x = 250 m

Island was well explained by this numerical simulation. The formation of the topography resembling a bell is due to the wave-sheltering effect of the island, and such a topography will disappear with the erosion of the island. Thus, the applicability of the BG model was confirmed.

CONCLUSION

The BG model was used to predict the deformation of a sandy island observed by performing a movable-bed experiment and the deformation of a volcanic island composed of ash and pumice, Taketomi Island, in the Okhotsk Sea. The predicted and measured topographic changes were in good agreement. Although the BG model has been used to predict the development of a river mouth bar, a single sand spit, the formation of sand spits on a coast with a sudden change in coastline, and the formation of a bay barrier (Serizawa and co-workers, 2009a, 2009b, 2011; Uda and Serizawa 2011), in this study, it was further applied to successfully predict the topographic changes around a sandy island in which shoreline instability may occur. Thus, the applicability of the BG model was further extended in this study. Because the calculation of nearshore currents is unnecessary in the BG model, the model has the practical advantage that the calculation can be performed without a large calculation load.

REFERENCES

Ashton, A., Murray, A. B. and Arnault, O. (2001). Formation of coastline features by large-scale instabilities induced by high angle waves, Nature, Vol. 414, pp. 296-300.

Dally, W. R., Dean, R. G. and Dalrymple, R. A. (1984). A model for breaker decay on beaches, Proc. 19th ICCE, pp. 82-97.

Goda, Y. (1985). Random Seas and Design of Maritime Structures, University of Tokyo Press, Tokyo, 323pp.

Mase, H. (2001). Multidirectional random wave transformation model based on energy balance equation, Coastal Eng. J., JSCE, Vol. 43, No. 4, pp. 317-337.

Ozasa, H. and Brampton, A. H. (1980). Model for predicting the shoreline evolution of beaches backed by seawalls, Coastal Eng., Vol. 4, pp. 47-64.

Serizawa, M., Uda, T., San-nami, T., Furuike, K. and Ishikawa, T. (2009a). Prediction of topographic changes of sand spit using BG model, J. Coastal Res., SI 56, pp. 1060-1064.

Serizawa, M., Uda, T., San-nami, T., Furuike, K. and Ishikawa, T. (2009b). Model for predicting recovery of a river mouth bar after flood using BG model, Asian and Pacific Coasts 2009, Proc. 5th Inter. Conf., Vol. 3, pp. 96-102.

Serizawa, M. and Uda, T. (2011). Prediction of formation of sand spit on coast with sudden change using improved BG model, Coastal Sediments '11, pp. 1907-1919.

Uda, T. and Yamamoto, K. (1991). Spit formation in lake and bay, Coastal Sediments '91, Vol. 2, pp. 1651-1665.

Uda, T. and Serizawa, M. (2011). Model for predicting formation of bay barrier in flat shallow sea, Coastal Sediments '11, pp. 1176-1189.

Zenkovich, V. P. (1967). Processes of Coastal Development, Interscience Publishers, New York, 751 pp.